V.P. KRAVCHUK

Bogolyubov Institute for Theoretical Physics, Nat. Acad. of Sci. of Ukraine
(14b, Metrolohichna Str., Kyiv 03680, Ukraine; e-mail: vkravchuk@bitp.kiev.ua)

STABILITY OF MAGNETIC NANOWIRES AGAINST SPIN-POLARIZED CURRENT

The stability of the ground magnetization state of a thin magnetic nanowire against a longitudinal spin-polarized current is studied theoretically with the dipole-dipole interaction taken into account. The critical current, i.e. the minimum current, at which the instability of the ground state develops, is determined. The dependence of the critical current on the size and the shape of a transversal wire cross-section is clarified. Theoretical predictions are confirmed by numerical micromagnetic simulations.

K e y w o r d s: magnetic nanowire, spin-current, spintronics, soliton.

1. Introduction

Magnetic wires, whose transversal size is small enough to ensure the magnetization variation only along the wire, are of high applied interest now. These one-dimensional magnetic systems are called nanowires, and they are considered to be convenient elements for nonvolatile data storage devices of a new type [1]. Sequence of bits of information in such a wire is coded by a sequence of magnetic domains magnetized along the wire. The magnetic domains are separated by the domain walls of head-to-head and tail-to-tail configurations [2]. Read-write processes require the motion of the domain sequence along the wire [1], what can be achieved by the passage of pulses of a spin-polarized current through the wire [1, 3, 4]. Recently, it was shown [5] that one can significantly increase the domain wall velocity by applying a spin-polarized current perpendicularly to the wire. Since the usage of a spin-polarized current is of high importance in this area, there arises the problem of stability of the uniform magnetization state against the current. Recently, we studied the stability of the uniformly magnetized nanowires against a perpendicular spin-polarized current [6]. The stability analysis in the case of longitudinal current was performed somewhat earlier [7]. However, the dipole-dipole interaction was neglected in Ref. [7]. In this paper, we present a linear theory of the stability of the ground state of a long nanowire against the longitudinal spin-polarized current with the dipole-dipole interaction taken into account. In contrast to the previous results [7], we will show that, due to the nonlocal nature of the dipole-dipole interaction, the shape and the size of a wire transversal cross-section affect the stability condition. The analytical predictions are checked by numerical micromagnetic simulations.

2. Model and Linearized Equation of Motion

Let us consider a rectilinear nanowire, whose length L much exceeds the characteristic transversal size. The wire is assumed to be narrow enough to ensure the magnetization uniformity in the transversal direction. In other words, we assume that the magnetization varies only along the wire. The magnetic medium is modeled as a discrete cubic lattice of magnetic moments $\boldsymbol{M_\nu}$, where $\nu = a(\nu_x, \nu_y, \nu_z)$ is a three-dimensional index, with a being the lattice constant and $\nu_x, \nu_y, \nu_z \in \mathbb{Z}$. It is convenient to introduce the following notation: $\mathcal{N}_z = L/a$ is the total number of lattice nodes along the z-axis oriented along the wire, and $\mathcal{N}_s$ is the number of nodes within the cross-section area.

Let the spin-polarized current with density $\boldsymbol{j} = j\hat{\boldsymbol{z}}$ pass through the wire. The magnetization dynamics in this system is described by a modified Landau–Lifshitz–Gilbert equation [4, 8, 9], which can be written in the following discrete form:

$$\dot{\boldsymbol{m}}_n = \left[\boldsymbol{m}_n \times \frac{\partial \mathcal{E}}{\partial \boldsymbol{m}_n}\right] + \alpha\left[\boldsymbol{m}_n \times \dot{\boldsymbol{m}}_n\right] -$$
$$- u\frac{\boldsymbol{m}_{n+a} - \boldsymbol{m}_n}{a} + u\beta\frac{\boldsymbol{m}_n \times \boldsymbol{m}_{n+a}}{a}. \qquad (1)$$

Here, the index $n = a\nu_z$ numerates the normalized magnetic moments $\boldsymbol{m}_n = \boldsymbol{M}_n/|\boldsymbol{M}_n|$ along the wire

axis, the overdot indicates the derivative with respect to the dimensionless time measured in units ω_0^{-1}, $\omega_0 = 4\pi\gamma M_s$ with γ being the gyromagnetic ratio, and M_s being the saturation magnetization. The quantity $\mathcal{E} = E/(4\pi M_s^2 a^3 \mathcal{N}_s)$ is the dimensionless total energy of the system. The normalized current is presented by the quantity $u = jP\hbar/(8\pi|e|M_s^2)$, which is close to the average electron drift velocity. Here, P is the value of spin polarization, $\hbar$ is the Planck constant, and e is the electron charge. Here, α is the Gilbert damping constant, and β is the nonadiabatic spin-transfer parameter.

The problem of action of the spin-polarized conducting electrons on the magnetization states nonuniform along the current direction was first discussed in Ref. [10]. The simple form of Eq. (1) without the nonadiabatic term was obtained in Ref. [8] within the ballistic transport model for half-metallic materials. In this case, the spin-wave instability of uniformly magnetized states was predicted for large currents [8, 11]. Later in Ref. [9], the nonadiabatic spin-transfer term was introduced. The micromagnetic analysis of Eq. (1) was provided in Ref. [4] with corresponding study of the current-driven domain wall motion (for a detailed derivation of spin-torques and the applications, see reviews [7, 12–14]).

In the following, we use the previously developed method [6, 15] based on the Holstein–Primakoff representation for spin operators [16] generalized by Tyablikov [17]. This method enables one to consider the dipole-dipole interaction exactly for linear [6, 18] as well as for weakly nonlinear [15] problems. In line with the aforementioned method, we introduce the complex amplitude ψ_n of a magnetization deviation from the ground state $\boldsymbol{m} = \hat{\boldsymbol{z}}$,

$$\psi_n = \frac{m_n^x + i\, m_n^y}{\sqrt{1 + m_n^z}}, \tag{2}$$

where m_n^x and m_n^y denote the magnetization components perpendicular to the wire. In terms of the amplitude $\psi_{\mathbf{n}}$, the linearized form of (1) reads

$$(1 - i\alpha)\dot{\psi}_n = i\frac{\partial \mathcal{E}^0}{\partial \psi_n^*} - u(1 - i\beta)\frac{\psi_{n+a} - \psi_n}{a}, \tag{3}$$

where $\mathcal{E}^0$ is the harmonic part of the total energy[1], for details see Appendix A.

---

[1] $\mathcal{E}^0$ includes terms not higher than $\mathcal{O}(|\psi_n|^2)$.

For the further analysis, it is convenient to proceed to the wave-vector space, because the energy $\mathcal{E}^0$ takes a relatively simple form in this case [6, 15], which enables us to proceed analytically. This is an advantage of the ψ-representation (2). We use the one-dimensional Fourier transform

$$\psi_n = \frac{1}{\sqrt{\mathcal{N}_z}}\sum_k \hat{\psi}_k e^{ikn}, \tag{4a}$$

$$\hat{\psi}_k = \frac{1}{\sqrt{\mathcal{N}_z}}\sum_n \psi_n e^{-ikn} \tag{4b}$$

with the orthogonality condition

$$\sum_n e^{i(k-k')n} = \mathcal{N}_z\Delta(k - k'), \tag{4c}$$

where $k = \frac{2\pi}{L}l$ is a two-dimensional discrete wave vector, $l \in \mathbb{Z}$, and $\Delta(k)$ is the Kronecker delta. Applying (4) to the linearized equation (3) and using the long-wave approximation $k \ll 2\pi/a$, one obtains

$$(1 - i\alpha)\dot{\hat{\psi}}_k = i\frac{\partial \mathcal{E}^0}{\partial \hat{\psi}_k^*} - uk(i + \beta)\hat{\psi}_k. \tag{5}$$

3. Energy of the System

We consider here the case of a soft ferromagnet; therefore, only two contributions to the total energy are taken into account: $E = E_{\mathrm{ex}} + E_{\mathrm{d}}$. Here,

$$E_{\mathrm{ex}} = -\mathcal{S}^2\mathcal{J}\sum_{\boldsymbol{\nu},\boldsymbol{\delta}}\boldsymbol{m}_{\boldsymbol{\nu}}\cdot\boldsymbol{m}_{\boldsymbol{\nu}+\boldsymbol{\delta}} \tag{6}$$

is the exchange contribution, where $\boldsymbol{\delta}$ numerates the nearest neighbors of an atom, $\mathcal{S}$ denotes the value of classical spin, and $\mathcal{J} > 0$ is the exchange integral between two nearest atoms. In terms of the Fourier components $\hat{\psi}_k$, the harmonic part of the normalized exchange energy reads

$$\mathcal{E}_{\mathrm{ex}}^0 = \ell^2\sum_k k^2|\hat{\psi}_k|^2, \tag{7}$$

where $\ell = \sqrt{\mathcal{S}^2\mathcal{J}/(2\pi M_s^2 a)}$ is the so-called exchange length. The value of ℓ determines a typical length-scale of magnetization inhomogeneities; for typical magnets, $\ell = 2$–10 nm [19]. The derivation of (7) is analogous to one presented in Appendix A1 of Ref. [15].

The other term is the dipole-dipole energy

$$E_{\mathrm{d}} = \frac{M_s^2 a^6}{2}\sum_{\boldsymbol{\nu}\neq\boldsymbol{\mu}}\left[\frac{(\boldsymbol{m}_{\boldsymbol{\nu}}\cdot\boldsymbol{m}_{\boldsymbol{\mu}})}{r_{\boldsymbol{\nu}\boldsymbol{\mu}}^3} - \right.$$

$$-3\frac{(\boldsymbol{m_\nu}\cdot\boldsymbol{r_{\nu\mu}})\,(\boldsymbol{m_\mu}\cdot\boldsymbol{r_{\nu\mu}})}{r_{\nu\mu}^5}\Bigg], \tag{8}$$

where we introduce the notation $\boldsymbol{r_{\nu\mu}} = (x_{\nu\mu}, y_{\nu\mu}, z_{\nu\mu}) = \boldsymbol{\mu} - \boldsymbol{\nu}$.

Since the magnetization depends only on the z-coordinate, one can write the harmonic part of the normalized dipole-dipole energy in the form

$$\mathcal{E}_{\mathrm{d}}^0 = \frac{1}{2}\sum_k \Big\{ [\hat{g}(k) + 2\hat{g}(0)]\,|\hat{\psi}_k|^2 -$$

$$- 3\hat{f}(k)\hat{\psi}_k\hat{\psi}_{-k} \Big\} + \text{c.c.} \tag{9a}$$

(see Appendix B for details). All information about the shape of a wire cross-section and its size is incorporated into the functions

$$\hat{g}(k) = \frac{a^3}{8\pi\mathcal{N}_s} \times$$

$$\times \sum_n \sum_{\mu_x,\mu_y\nu_x,\nu_y} \frac{2n^2 - x_{\nu\mu}^2 - y_{\nu\mu}^2}{\left(x_{\nu\mu}^2 + y_{\nu\mu}^2 + n^2\right)^{5/2}} e^{ikn}, \tag{9b}$$

$$\hat{f}(k) = \frac{a^3}{8\pi\mathcal{N}_s} \times$$

$$\times \sum_n \sum_{\mu_x,\mu_y\nu_x,\nu_y} \frac{(x_{\nu\mu} - iy_{\nu\mu})^2}{\left(x_{\nu\mu}^2 + y_{\nu\mu}^2 + n^2\right)^{5/2}} e^{ikn}. \tag{9c}$$

Here, we use the notation $x_{\nu\mu} = a(\mu_x - \nu_x)$ and $y_{\nu\mu} = a(\mu_y - \nu_y)$ for the sake of simplicity.

Let us consider a nanowire in the form of a tube with inner and outer radii ρ and R, respectively. Applying the transition from summation to integration with the singularity extraction (see Appendix B in Ref. [6]), one obtains

$$\hat{f}(k)\Big|_{\mathrm{tube}} = 0,$$

$$\hat{g}(k)|_{\mathrm{tube}} = \frac{1}{R^2 - \rho^2}\Big[R^2 \mathrm{I}_1(Rk)\mathrm{K}_1(Rk) - \tag{10}$$

$$- 2R\rho\mathrm{I}_1(\rho k)\mathrm{K}_1(Rk) + \rho^2 \mathrm{I}_1(\rho k)\mathrm{K}_1(\rho k) \Big] - \frac{1}{3},$$

where $\mathrm{I}_1(x)$ and $\mathrm{K}_1(x)$ are the modified Bessel functions of the first and second kinds, respectively [20]. In the limit case of cylindrical wire ($\rho \to 0$), one obtains

$$\hat{g}(k)|_{\mathrm{cyl}} = \mathrm{I}_1(Rk)\mathrm{K}_1(Rk) - \frac{1}{3}. \tag{11}$$

Finally, the harmonic part of the dipole-dipole energy of a cylindrical nanowire reads

$$\mathcal{E}_{\mathrm{d}}^0\Big|_{\mathrm{cyl}} = \sum_k \mathrm{I}_1(Rk)\mathrm{K}_1(Rk)|\hat{\psi}_k|^2. \tag{12}$$

It should be noted that, in the case of a nanowire with square cross-section, the dipole-dipole energy has a similar form [6]

$$\mathcal{E}_{\mathrm{d}}^0\Big|_{\mathrm{sqr}} \approx \sum_k \mathrm{I}_1\left(hk/\sqrt{\pi}\right)\mathrm{K}_1\left(hk/\sqrt{\pi}\right)|\hat{\psi}_k|^2, \tag{13}$$

where h is the side of the square cross-section.

3.1. Effective Anisotropy Approach

Here, we discuss a possibility to model the nanowire dipole-dipole energy by an easy axis anisotropy with the axis oriented along the wire:

$$E_{\mathrm{an}} = -\frac{K}{2}\sum_\nu (m_\nu^z)^2, \quad K > 0. \tag{14}$$

In the wave-vector space, the harmonic part of the normalized energy (14) reads

$$\mathcal{E}_{\mathrm{an}}^0 = \kappa \sum_k |\hat{\psi}_k|^2, \tag{15}$$

where $\kappa = K/(4\pi M_s^2 a^3)$. Comparing (15) and (9a), one concludes that the anisotropy constant for a round nanowire is effectively $\kappa = \hat{g}(k) + 2\hat{g}(0)$. Within the long-wave approximation $kR \ll 1$ or, in other words, assuming that the characteristic size of a magnetization nonuniformity exceeds considerably the transversal size of the wire, we obtain $\kappa \approx 3\hat{g}(0)$. In the case of a tubular or cylinder shaped nanowire, expression (10) yields the anisotropy constant $\kappa \approx 1/2$. A few remarks should be made: (i) In the case of a tubular wire with thin wall ($\rho \approx R$), the simple form of anisotropy (14) is insufficient, and an additional easy-surface anisotropy term should be introduced. However, this type of anisotropy cannot be considered within the one-dimensional model which is used here, and this discussion is beyond the scope of this paper. (ii) Accordingly to (13) for a wire with square cross-section, the effective anisotropy has the same value $\kappa \approx 1/2$.

4. Linear Instability Analysis

We now substitute the energy expression $\mathcal{E}^0 = \mathcal{E}_{\mathrm{ex}}^0 + \mathcal{E}_{\mathrm{d}}^0$, where the exchange $\mathcal{E}_{\mathrm{ex}}^0$ and dipole-dipole $\mathcal{E}_{\mathrm{d}}^0$ contributions are determined by (7) and (9a), respectively, into Eq. (5). Equation (5) and its complex
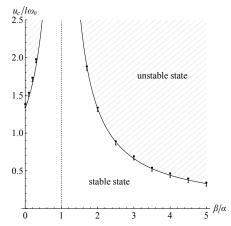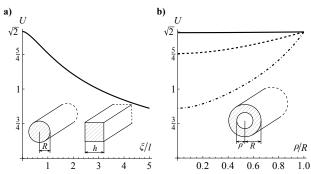
Fig. 1. Stability region for a wire with square cross-section with $h/\ell = 1.13$ (corresponds to $h = 6$ nm for permalloy). Solid line shows the critical current u_c obtained from (19) and (20). The transition to an instability obtained with micromagnetic simulations is shown by verticals bars: at the top point and higher, the instability is developed, at the bottom point and lower, the state is stable

Fig. 2. Dependence of the shape parameter U on the shape and the size of a wire cross-section. Inset *a*) corresponds to the wires of round ($\xi = R$) and square ($\xi = h/\sqrt{\pi}$) cross-sections. Inset *b*) corresponds to the tubular wire with different outer radii: solid line – $R/\ell = 0.1$, dashed line – $R/\ell = 1$, dot-dashed line – $R/\ell = 5$

conjugated form compose a set of two linear equations for the functions $\hat{\psi}_k$ and $\hat{\psi}^*_{-k}$. The corresponding solutions are

$$\hat{\psi}_k = \Psi_+ e^{z_+(k)t}, \quad \hat{\psi}^*_{-k} = \Psi_- e^{z_-(k)t}, \quad (16a)$$

where $\Psi_\pm$ are constants, and the rate functions $z_\pm(k)$ are determined as

$$(1 + \alpha^2)z_\pm = -\alpha\Omega - iuk(1 + \alpha\beta) \pm$$
$$\pm \sqrt{[i\Omega + uk(\alpha - \beta)]^2 + (1 + \alpha^2)\varpi^2}, \quad (16b)$$

1004

where we introduced the notation

$$\Omega = \ell^2 k^2 + \hat{g}(k) + 2\hat{g}(0), \quad (16c)$$

$$\varpi = \frac{3}{2}\left|\hat{f}(k) + \hat{f}(-k)\right|. \quad (16d)$$

The instability condition for the system can be written as

$$\exists k : \Re z_\pm(k) > 0. \quad (17)$$

In what follows, we consider the case $\varpi = 0$, which corresponds to nanowires with symmetric cross-sections: cylindrical rods, tubular and square nanowires. In this case, the rate function has more simple form

$$z_\pm(k) = \frac{\gamma_\pm(k) \pm i\omega_\pm(k)}{1 + \alpha^2}, \quad (18a)$$

where

$$\gamma_\pm(k) = -\alpha\left[\Omega(k) \pm uk\left(1 - \frac{\beta}{\alpha}\right)\right], \quad (18b)$$

$$\omega_\pm(k) = \Omega(k) \mp uk(1 + \alpha\beta). \quad (18c)$$

The last term in (18c) represents the Doppler shift [7, 21] induced by the spin current.

The instability condition (17) can be written now as $\gamma_\pm > 0$ or, equivalently,

$$|u| > u_c = \frac{U}{|1 - \beta/\alpha|}, \quad U = \min_{k>0}\frac{\Omega(k)}{k}. \quad (19)$$

The law $u_c \propto |1 - \beta/\alpha|^{-1}$ was already obtained [7] for anisotropic nanowires, where the dipole-dipole contribution was neglected. In contrast to the previous results, expression (19) involves the shape and the transversal size of a wire which are incorporated into the shape parameter U.

As an example, we consider a nanowire with square cross-section with side h. In this case,

$$\Omega(k) = \ell^2 k^2 + I_1\left(hk/\sqrt{\pi}\right) K_1\left(hk/\sqrt{\pi}\right). \quad (20)$$

The corresponding instability area determined by (19) is shown in Fig. 1.

The noticeable dependence of the shape parameter U on the shape and the size of the wire cross-section is demonstrated in Fig. 2.

To check the obtained stability condition (19), we perform full scale micromagnetic simulations [22]. We simulate the magnetization dynamics induced by the

spin-current passing along a square nanowire with $h = 6$ nm and $L = 1\,\mu$m. The periodic boundary conditions are implemented along the wire. We choose the following material parameters of permalloy: the saturation magnetization $M_s = 8.6 \times 10^5$ A/m, and the exchange length $\ell = 5.3$ nm (this corresponds to the exchange constant $A = 1.3 \times 10^{-11}$ J/m). The anisotropy is neglected. The characteristic time scale is determined by the uniform ferromagnetic resonance frequency $\omega_0 = 1.9 \times 10^{11}$ rad/s (30.3 GHz). The value of damping constant $\alpha = 0.01$ is close to the natural one. For permalloy, the nonadiabatic spin-transfer parameter is $\beta = 0.04$ [4]. However, we vary it in the range $0 \leq \beta/\alpha \leq 5$ in order to check the instability condition (19), see Fig. 1. The discretization mesh is a cubic one: $\Delta x = \Delta y = \Delta x = 3$ nm. The initial state is a slightly noised ground state $\boldsymbol{m}_{\mathrm{ini}} = \tilde{\boldsymbol{m}}/|\tilde{\boldsymbol{m}}|$, where $\tilde{\boldsymbol{m}} = (\tilde{m}_x, \tilde{m}_y, 1)$ with transverse components $|\tilde{m}_x| < 10^{-4}$ and $|\tilde{m}_y| < 10^{-4}$, being determined in a random way. For a certain current value u, the magnetization dynamics is simulated during the long time $\Delta t = 100$ ns ($\sim 10^2 \omega_0^{-1}\alpha^{-1}$). The judgement about the stability is based on the time dependence of the total energy $E(t)$: if $E(t)$ exponentially decays, then the ground state of the wire is considered to be stable for the given current u, and if the dependence $E(t)$ start to rise, then the decision about instability is made. Results of the described stability analysis are shown in Fig. 1 by vertical bars: at the top point of the bar and higher, the instability is developed; at the bottom point and lower, the state is stable. One can see a nice agreement of the numerical results with the theoretical prediction (19).

In summary, we show that the dipole-dipole interaction noticeably changes the stability condition of the nanowire ground state with respect to the spin-current. The shape and the size of the wire cross-section affect the instability condition due to the non-local nature of the dipole-dipole interaction.

APPENDIX A
Equation of motion in terms of amplitude ψ

Considering $\boldsymbol{m}_n = \boldsymbol{m}_n(\psi, \psi^*)$, we project Eq. (1) onto the transversal axes x and y. Solving the obtained set of equations

for $\dot{\psi}$ and $\dot{\psi}^*$, one obtains

$$(1 + \alpha^2)\dot{\psi}_n = i\frac{\partial\mathcal{E}}{\partial\psi_n^*}\,(1 + i\alpha\Psi_+) -$$
$$- u\frac{\psi_{n+a} - \psi_n}{a}\,[1 + \alpha\beta + i(\alpha - \beta)\Psi_+] +$$
$$+ \frac{\psi_n^2}{|\psi_n|^2}\Psi_-\left[\alpha\frac{\partial\mathcal{E}}{\partial\psi_n} + iu(\alpha - \beta)\frac{\psi_{n+a}^* - \psi_n^*}{a}\right],$$

$$\Psi_\pm = \frac{1}{2}\left(\frac{2 - |\psi_n|^2}{2} \pm \frac{2}{2 - |\psi_n|^2}\right). \tag{A1}$$

For details, see Appendix A of Ref. [6]. The linearization of (A1) with respect to ψ_n results in (3).

APPENDIX B
Dipole-dipole interaction for 1D case

As a direct consequence of the dependence of the magnetization on the longitudinal coordinate z only, the dipole-dipole energy (8) can be presented in the form

$$E_{\mathrm{d}} = \frac{M_s^2 a^6}{2}\sum_{\nu_z, \mu_z}\left[\sum_{\varsigma = x, y, z}\mathcal{A}_{\nu_z\mu_z}^\varsigma m_{\nu_z}^\varsigma m_{\mu_z}^\varsigma +\right.$$
$$\left.+ \mathcal{B}_{\nu_z\mu_z} m_{\nu_z}^x m_{\mu_z}^y\right], \tag{B1a}$$

where the summation over the transversal dimensions is enclosed in the coefficients

$$\mathcal{A}_{\nu_z\mu_z}^\varsigma = \sum_{\substack{\mu_x, \mu_y \\ \nu_x, \nu_y \\ \boldsymbol{\nu} \neq \boldsymbol{\mu}}}\frac{r_{\boldsymbol{\nu\mu}}^2 - 3\varsigma_{\boldsymbol{\nu\mu}}^2}{r_{\boldsymbol{\nu\mu}}^5},$$

$$\mathcal{B}_{\nu_x\mu_x} = -6\sum_{\substack{\mu_x, \mu_y \\ \nu_x, \nu_y \\ \boldsymbol{\nu} \neq \boldsymbol{\mu}}}\frac{y_{\boldsymbol{\nu\mu}} z_{\boldsymbol{\nu\mu}}}{r_{\boldsymbol{\nu\mu}}^5}. \tag{B1b}$$

Substituting now the magnetization components

$$m_n^z = 1 - |\psi_n|^2$$
$$m_n^x \approx \frac{\psi_n + \psi_n^*}{\sqrt{2}}, \quad m_n^y \approx \frac{\psi_n - \psi_n^*}{i\sqrt{2}} \tag{B2}$$

into (B1) and applying the Fourier transformation (4), one obtains the harmonic part of the normalized dipole-dipole energy in form (9).

1. S.S.P. Parkin, M. Hayashi, and L. Thomas, Science **320**, 190 (2008).
2. M. Kläui, J. of Phys.: Cond. Mat. **20**, 313001 (2008).
3. M. Kläui, P.-O. Jubert, R. Allenspach, A. Bischof, J.A.C. Bland, G. Faini, U. Rüdiger, C.A.F. Vaz, L. Vila, and C. Vouille, Phys. Rev. Lett. **95**, 026601 (2005).
4. A. Thiaville, Y. Nakatani, J. Miltat, and Y. Suzuki, Europhys. Lett. **69**, 990 (2005).
5. A.V. Khvalkovskiy, K.A. Zvezdin, Y.V. Gorbunov, V. Cros, J. Grollier, A. Fert, and A.K. Zvezdin, Phys. Rev. Lett. **102**, 067206 (2009).

6. V.P. Kravchuk, O.M. Volkov, D.D. Sheka, and Y. Gaididei, Phys. Rev. B **87**, 224402 (2013).
7. Y. Tserkovnyak, A. Brataas, and G.E. Bauer, J. of Magn. Magn. Mater. **320**, 1282 (2008).
8. Y.B. Bazaliy, B.A. Jones, and S.-C. Zhang, Phys. Rev. B **57**, R3213 (1998).
9. S. Zhang and Z. Li, Phys. Rev. Lett. **93**, 127204 (2004).
10. L. Berger, J. Appl. Phys. **49**, 2156 (1978).
11. Z. Li and S. Zhang, Phys. Rev. Lett. **92**, 207203 (2004).
12. D. Ralph and M. Stiles, J. Magn. Magn. Mater. **320**, 1190 (2008).
13. G. Tatara, H. Kohno, and J. Shibata, Phys. Reports **468**, 213 (2008).
14. A. Brataas, A.D. Kent, and H. Ohno, Nat. Mater. **11**, 372 (2012).
15. Y. Gaididei, O.M. Volkov, V.P. Kravchuk, and D.D. Sheka, Phys. Rev. B **86**, 144401 (2012).
16. T. Holstein and H. Primakoff, Phys. Rev. **58**, 1098 (1940).
17. S.V. Tyablikov, *Methods in the Quantum Theory of Magnetism* (Plenum Press, New York, 1967)].
18. A. Volkov and V. Kravchuk, Ukr. J. of Phys. **58**, 667 (2013).
19. R. Skomski, J. Phys. C **15**, R841 (2003).
20. F.W.J. Olver, D.W. Lozier, R.F. Boisvert, and C.W. Clark, eds., *NIST Handbook of Mathematical Functions* (Cambridge Univ. Press, New York, 2010).
21. J. Fernandez-Rossier, M. Braun, A.S. Nunez, and A.H. MacDonald, Phys. Rev. B **69**, 174412 (2004).
22. *The Object Oriented MicroMagnetic Framework*, developed by M.J. Donahue and D. Porter mainly, from NIST. We used the $1.2\alpha5$ release, URL `http://math.nist.gov/oommf/`.

В.П. Кравчук

СТІЙКІСТЬ МАГНІТНИХ
НАНОДРОТІВ ПО ВІДНОШЕННЮ
ДО СПІН-ПОЛЯРИЗОВАНОГО СТРУМУ

Р е з ю м е

Теоретично досліджено стійкість основного стану магнітних нанодротів по відношенню поздовжнього спін-поляризованого струму з урахуванням диполь-дипольної взаємодії. Визначено значення критичного струму – мінімального струму, при якому розвивається нестійкість. Продемонстровано залежність критичного струму від розміру та форми поперечного перерізу дроту. Теоретичні передбачення підтверджено чисельними мікромагнітними моделюваннями.